Sub-nanosecond optical diagnostics of streamer discharges

T. Hoder[1], D. Loffhagen[2], R. Brandenburg[2], Z. Bonaventura[1] and M. Šimek[3]

[1]*Masaryk University, Faculty of Science, Kotlarska 2, Brno 611 37, Czech Republic*
[2]*Leibniz Institute for Plasma Science and Technology (INP Greifswald), Felix-Hausdorff-Str. 2, 17489 Greifswald, Germany*
[3]*Department of Pulse Plasma Systems, Institute of Plasma Physics, Academy of Sciences of the Czech Republic, Za Slovankou 3, 182 00 Prague, Czech Republic*

Discharges in air frequently include a mechanism called streamer within their development. In this contribution, several issues concerning the optical diagnostics of such discharges are discussed. Particularly, the importance of the high spatial and temporal resolution of the detecting device on the quantitative experimental outputs is emphasized. The fundamental limits given by the relaxation times of the electron velocity distribution function or characteristic times of the quenching of excited states under given condition are also considered. Selected high-resolution recordings of early-stage streamers in corona or barrier discharges are taken as an example and the observed general phenomena are clarified using appropriate numerical modelling.

1. Introduction

Discharges in air frequently include a mechanism called streamer within their development. A streamer in air is a contracted ionizing wave that propagates into a weakly ionized or neutral medium exposed to a high electric field. It is characterized by a self-generated field enhancement at the head of the growing discharge channel leaving a trail of filamentary plasma behind. Such a wave phenomenon results from the space charge left by electron avalanches [1,2]. This mechanism is still present whether the discharge occurs in small millimetre or centimetre sized gaps of dielectric barrier discharges or coronas in laboratory at atmospheric pressure [3-5] or on large spatial scales at reduced pressures in the upper atmosphere within so-called transient luminous events (TLEs) [6,7].

A usual method to study these events consists in the use of high-speed cameras: frame cameras for TLEs and nanosecond-gated intensified CCD (ICCD) cameras for laboratory discharges. Nevertheless, if one takes into account the fact that the velocity of streamers under certain conditions reaches up to few percent of the speed of light, the nanosecond resolution of these cameras will not be high enough. It will certainly not be high enough to resolve the inner structure of the emission emitted by the streamer.

Recently, the papers of Celestin, Bonaventura and Naidis [7-9] contributed significantly to the understanding which information is given by the emission of the streamer if recorded by nanosecond-gated ICCD camera. Particularly, these papers addressed the consequences for the estimation of the electric field by the known method of ratio of two spectral bands of molecular nitrogen, i.e. the first negative system (FNS) of the molecular nitrogen ion with 0-0 transition and head maximum at 391.5 nm and the second positive system (SPS) of molecular nitrogen with transition 0-0 and head at 337.1 nm [10].

As a result of the above-mentioned introduction, this contribution discusses the inner structure of the streamer as it can be revealed by high-resolution measurements, addresses appropriate conditions for obtaining signal from plasma in local equilibrium, i.e. the excitation happens under stable conditions at a selected place and a certain time, and deals with the influence of the different values of effective lifetimes, i.e. the sufficiency of the speed of de-excitation of the radiative states.

2. Experimental setups

Three experimental discharge setups are included in this contribution – two of them at atmospheric pressure and one at pressures similar to TLE conditions, all in dry air.

At atmospheric pressure, the asymmetric barrier discharge and negative corona in Trichel pulse regime were analysed [11]. The gap width was 1 mm between stainless steel and by alumina-covered electrodes for the barrier discharge setup. The applied voltage was sinusoidal at a frequency of 60 kHz and peak-to-peak amplitude of 11 kV. The corona setup consisted of a grounded cathode with a tip curvature of 190 μm and a positive dc voltage (7.8 kV) connected plate, both made of stainless steel with a gap of 7 mm. This setup resulted in pulses with a frequency of approximately 200 kHz. The time-correlated single photon counting based spectroscopy device was applied as diagnostic technique. The achieved resolution of the discharge emission intensity was in the scale of tens of picoseconds and tens of micrometres.

In the case of the measurements at reduced pressure, the repetitive streamer event was generated in a symmetric dielectric-barrier-discharge geometry, where both electrodes with mutual distance of 40 mm were covered by dielectric material. One electrode was powered by repetitive high-voltage bursts (superimposing two sine-waves, f_{AC} = 1 kHz, with a positive pulse of a duration of 100 ns) at fixed repetition frequency of 30 Hz [12]. Light emitted by the streamer was recorded using a fast Hamamatsu photomultiplier (H10721) with temporal resolution of 200 ps.

3. Inner structure of a streamer

Measuring streamer emission of the FNS and the SPS system with high resolution, the following phenomenon can be revealed. The intensity maxima of FNS or SPS in time are delayed behind the maximum of the electric field of the streamer [9,11]. The value of these delays can reach up to 400 ps in the streamer development. As shown in [11], the detected emission just represents populations of excited states formed behind the running streamer head, giving only delayed information about the streamer head position. In [11], the equation

$$t_{delay} = (1-E_{delay}/E_{max})l_{axial}/2v_{streamer} \qquad (1)$$

describing this delay by other streamer parameters was derived, where t_{delay} is the time interval of the delay of the intensity signal maximum behind the maximum of the streamer electric field, E_{delay} and E_{max} are the electric field values at this delayed time coordinate and the streamer peak electric field value, respectively, l_{axial} is the axial length of the streamer [9,13] and $v_{streamer}$ is the streamer velocity. One can see from (1) that the value of the delay for the FNS or SPS emission intensity is directly linked to the fundamental streamer parameters. Thus, one gets an additional parameter to reconstruct the streamer structure from measurable quantities together with the velocity-diameter relation to the electric field value of the streamer [9] and a similar relation for the streamer current [14].

4. Relaxation of electron velocity distribution function

In order to justify the use of the hydrodynamic equilibrium approximation by measurements with such a high temporal and spatial resolution, different approaches can be used. One approach consists in the analysis of the energy-resolved collision frequencies for momentum and energy dissipation as well as the energy-resolved mean free path and energy dissipation length and it can already be done on the basis of known electron collision cross section data. If both the dissipation frequencies are larger than the frequency of electric field variation and both the characteristic lengths are smaller than the length of electric field change for all relevant kinetic energies U of the electrons, the electrons are in equilibrium with the electric field. The fulfillment of these relations was shown for the corona discharge in air at atmospheric pressure in [5].

Another approach is the study of the electron relaxation in time and space for different reduced electric field strengths E/N. Using again the electron collision cross sections for air, the temporal and/or spatial relaxation of the electrons can be determined by solving the electron Boltzmann equation (EBE) or by Monte Carlo (MC) simulations.

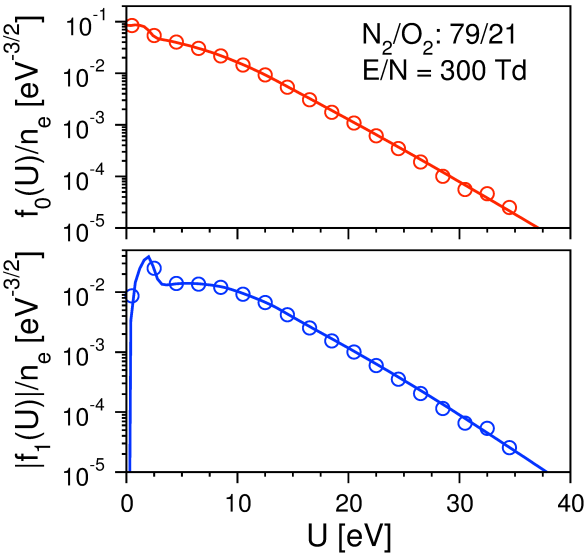

Fig. 1: Electron velocity distribution function components calculated for synthetic air at standard conditions and reduced electric field of 300 Td. The lines denote the temporally relaxed components after 10 ps and the circles are the spatially relaxed functions after 5 µm.

Figure 1 shows results for the isotropic (f_0) and first anisotropic (f_1) component of the electron velocity distribution function (EVDF) normalized by the electron density n_e obtained for E/N = 300 Td. The lines represent both these components after 10 ps of the temporal electron relaxation determined from the solution of the EBE in multi-term approximation. The symbols denote f_0 and f_1 calculated for the spatial relaxation (in one dimension) of the electrons after a distance of 5 µm using the MC method. The EBE and MC results agree well and coincide as well with the corresponding steady-state electron distribution function components. Thus, equilibrium values are reached after 10 ps and 5 µm.

5. Issues of quenching

Analysing the streamer emission, one has to take into account also the influence of the quenching, i.e. the resulting effective lifetimes of the excited states of emitting species [15,16]. Especially, in the case of the determination of the electric field from the ratio of the FNS and SPS signals, one has to consider the "proper" values, or better to say, to be aware of possible complications by taking different quenching time values into account [17,18].

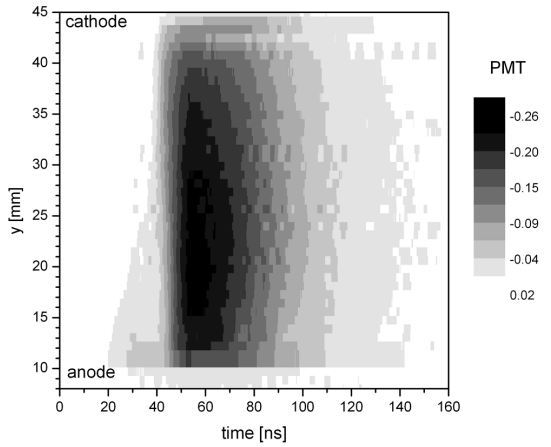

Fig. 2: SPS emission of the barrier discharge in air at a pressure of 10 Torr. Creation of the cathode layer and transient positive column is well visible.

In some cases where the changes in the discharge dynamics (excitation processes) happen on time scales comparable to the effective lifetimes or shorter, it can be a fundamental limitation to determine correct local values of selected quantities from this emission.

In the case of low-pressure streamer discharges, it is possible to determine the correct values of the peak electric field in the streamer head by including the differential nature of the equations for the kinetic scheme applied for the estimation of the electric field from the ratio of FNS and SPS intensities. This assumes of course having high-resolution spectroscopic recordings for disposal.

In Figure 2, the axial profile of the barrier discharge SPS emission in air at a pressure of 10 Torr is shown, scanned by a high-speed photomultiplier. The first contour appearing between 20 and 45 ns represents the accelerated ionization in the volume reaching a maximal velocity of 8×10^6 m/s close to the cathode. From this streamer propagation given by the SPS signal, we selected a single coordinate and added a similar measurement for the FNS. In this way, the local electric field development in time was determined using a similar approach as in [5] as a representative case. Varying the relevant effective lifetimes for the $N_2(C^3\Pi_u)$ and $N^+_2(B^2\Sigma^+_u)$ states within the order of magnitude, we obtained still the same peak electric field value for the streamer head within negligible error interval.

6. Summary

Obviously, optical diagnostics performed with enhanced spatio-temporal resolutions (micrometers, picoseconds) offer deeper experimental insight into the internal structure of streamers. However, additional issues as e.g. sufficient EVDF relaxation or slow quenching of radiative states have to be taken into account for the proper interpretation and discussion of high-resolved recordings. In the future, SPS emissions for higher vibrational levels ($v > 0$) as indicators for lower fields behind the streamer-head maxima should be addressed or waveforms of the strongest bands of the first positive system (FPS), the Herman infrared (HIR) system, the Gamma (γ) system of NO, and selected lines of atomic transitions should be investigated with high resolution [15].

Acknowledgment

The work was partly supported by the Federal German Ministry of Education and Research (BMBF) under grant FKZ 03FO1072. ZB acknowledges support by the Czech Science Foundation research project 15-04023S. TH acknowledges support by the ESF Research Networking Programme entitled 'Thunderstorm effects on the atmosphere-ionosphere system' within the exchange grant nr. 4219.

References

[1] U. Ebert, C. Montijn, T. M. P. Briels, W. Hundsdorfer, B. Meulenbroek, A. Rocco, and E. M. van Veldhuizen, *Plasma Sources Sci. Technol.* **15** (2006) S118–S129.

[2] E. Marode, D. Djermoune, P. Dessante, C. Deniset, P. Segur, F. Bastien, A. Bourdon, and C. Laux, *Plasma Phys. Control. Fusion* **51** (2009) 124002.

[3] H. Höft, M. Kettlitz, M. M. Becker, T. Hoder, D. Loffhagen, R. Brandenburg, and K.-D. Weltmann, *J. Phys. D: Appl. Phys.* **47** (2014) 465206.

[4] M. M. Nudnova and A. Yu. Starikovskii, *J. Phys. D: Appl. Phys.* **41** (2008) 234003.

[5] T. Hoder, M. Cernak, J. Paillol, D. Loffhagen, and R. Brandenburg, *Phys. Rev. E* **86** (2012) 055401.

[6] V. P. Pasko *Plasma Sources Sci. Technol.* **16** (2007) S13–S29.

[7] S. Celestin and V. P. Pasko, *Geophys. Res. Lett.* **37** (2010) L07804.

[8] Z. Bonaventura, A. Bourdon, S. Celestin, and V.

Pasko, *Plasma Sources Sci. Technol.* **20** (2011) 035012.
[9] G. V. Naidis, *Phys. Rev. E* **79** (2009) 057401.
[10] P. Paris, M. Aints, F. Valk, T. Plank, A. Haljaste, K. V. Kozlov, and H.-E. Wagner, *J. Phys. D: Appl. Phys.* **38** (2005) 3894–3899.
[11] T. Hoder, Z. Bonaventura, A. Bourdon, and M. Šimek, *J. Appl. Phys.* **117** (2015) 073302.
[12] M. Šimek, P. F. Ambrico, V. Prukner, *J. Phys. D: Appl. Phys.* **46** (2013) 485205.
[13] A. Kulikovsky, *Phys. Rev. E* **57** (1998) 7066.
[14] G. B. Sretenović, I. B. Krstić, V. V. Kovačević, B. M. Obradović, and M. M. Kuraica, *J. Phys. D: Appl. Phys.* **47** (2014) 355201.
[15] M. Šimek, *J. Phys. D: Appl. Phys.* **47** (2014) 463001.
[16] G. Dilecce, *Plasma Sources Sci. Technol.* **23** (2014) 015011.
[17] G. Dilecce, P. F. Ambrico, and S. DeBenedictis, *J. Phys. D: Appl. Phys.* **43** (2010) 195201.
[18] F. Valk, M. Aints, P. Paris, T. Plank, J. Maksimov, and A. Tamm, *J. Phys. D: Appl. Phys.* **43** (2010) 385202.